Two channel wavefront sensor arrangement employing moiré deflectometry

Saifollah Rasouli[a], Anamparambu N. Ramaprakash[b], H. K. Das[b], C. V. Rajarshi[b], Yasser Rajabi[a], and M. Dashti[a]

[a]Institute for Advanced Studies in Basic Sciences, Gava Zang, Zanjan 45195-1159, IRAN;
[b]Inter-University Centre for Astronomy and Astrophysics, Post Bag 4, Ganeshkhind, Pune - 411 007, INDIA

ABSTRACT

A wavefront sensor which takes advantage of the moiré deflectometry has been constructed for measuring atmosphere induced wavefront distortions. In this sensor a collimated laser beam propagates through turbulent atmosphere, then a beam splitter splits it into two beams and the beams pass through a pair of moiré deflectometers. Directions of the grating's rulings are parallel in each moiré deflectometer but are perpendicular in the two beams. Using a suitable array of lenses and mirrors two sets of moiré patterns are projected on a CCD camera. A suitable spatial filter removes the unwanted frequencies. Recording the successive moiré patterns by the CCD camera and feeding them to a computer, allow temporal fluctuations of the laser beam wavefront phase to be measured highly accurately. Displacements of the moiré fringes in the recorded patterns correspond to the fluctuations of two orthogonal components of the angle of arrival (AA) across the wavefront. The fluctuations have been deduced in successive frames, and then evolution of the wavefront shape is determined. The implementation of the technique is straightforward and it overcomes some of the technical difficulties of the Schlieren and Shack-Hartmann techniques. The sensitivity of detection is adjustable by merely changing the distance between two gratings in both moiré deflectometers and relative grating ruling orientation. This overcomes the deficiency of the Shack-Hartman sensors in that these require expensive retrofitting to change sensitivity. Besides, in the moiré deflectometry, the measurement is relatively insensitive to the alignment of the beam into the device. Hence this setup has a very good potential for adaptive optics applications in astronomy. Since tilts are measured in the Shack-Hartmann method at discrete locations, it cannot detect discontinuous steps in the wavefront. By this method discontinuous steps in the wavefront are detectable, because AA fluctuations are measured across the wavefront.

Keywords: wavefront sensing, atmospheric turbulence, laser beam propagation, moiré deflectometry, self-imaging phenomenon

1. INTRODUCTION

Moiré deflectometry is a well-known technique used to measure ray deflections when traveling through a phase object, based on the moiré and Talbot effects.[1] Talbot effect and moiré deflectometry have been used for wavefront sensing in different fields.[2–6] Other techniques, such as Shack-Hartmann[7] and Schlieren[8] methods are also used for wavefront sensing. The Shack-Hartmann sensor is often used for the measurement of turbulence-induced phase distortions for various applications in atmospheric studies and adaptive optics. As far as we know moiré deflectometry has not been used for sensing wavefronts propagating through a turbulent atmosphere.

A typical moiré deflectometry setup uses two linear, ruled, gratings of opaque lines which are separated by a distance, Z_k. The incoming beam of light is normal to both the gratings. The parameter Z_k denotes the kth self-image or Talbot's distance. In practice, the incident (often non-planar) wavefront hits the first grating,

Further author information: (Send correspondence to S. Rasouli)
S. Rasouli: E-mail: rasouli@iasbs.ac.ir, Telephone: +98 241 415 2062
A. N. Ramaprakash: E-mail: anr@iucaa.ernet.in, Telephone: +91 20 2569 4100

Optics in Atmospheric Propagation and Adaptive Systems XII, edited by Anton Kohnle, Karin Stein, John D. Gonglewski,
Proc. of SPIE Vol. 7476, 74760K · © 2009 SPIE · CCC code: 0277-786X/09/$18 · doi: 10.1117/12.829962

$G1$, so that after propagation over the distance Z_k between the gratings, the superposition of the first grating's self-image with grating $G2$ produces (distorted) moiré fringes. For a small angle between grating rulings θ, the moiré fringe direction is roughly perpendicular to both sets of grating rulings. If the rulings of the gratings are in the x direction, the deflectometer is not sensitive to wavefront changes in the x-axis direction, but only in the y-direction.

The use of a crossed grating for the simultaneous acquisition of two independent pieces of information is a known procedure in shearing interferometry and experimental mechanics. Such crossed ruling grids make it possible to process two orthogonal ray deflections at the same time. The two tilts of the wavefront, in the x and y directions can thus be examined simultaneously by using two dimensional gratings. But such use of crossed gratings lead to some difficulties in the Fourier plane and intensity losses.

In this work we used one pair of identical moiré deflectometers. A collimated laser beam propagates through turbulent atmosphere, then a beam splitter splits it into two beams and each beam passes through a distinct moiré deflectometer. Directions of the grating's rulings are parallel in each moiré deflectometer but are perpendicular in the two beams. Using a suitable array of lenses and mirrors two sets of moiré patterns are projected on a CCD camera. Displacements of the moiré fringes in these patterns correspond to the fluctuations of two components of the angle of arrival across the wavefront.

2. THEORETICAL CONSIDERATION

In a moiré deflectometer that consists of one dimensional gratings, when the direction of the grating rulings are in x-direction, the deflectometer is sensitive to wavefront changes only in the y-direction. In this work, we have used two moiré deflectometer channels, in which for the first channel, the grating rulings are roughly in the x-direction. In the second channel, the grating rulings are roughly in the y-direction.

In both channels, the changes in the moiré patterns are related to the distance between gratings in the experimental setup Z_k, the angle between grating rulings θ in each moiré deflectometer, and the ray deflections - the corresponding component of the angle of arrival fluctuations (AA) - of the incident wavefront. These fluctuations can be related with the normal direction of the emerging wavefront.

For each channel, the expected changes in the moiré pattern can be obtained as follows: assuming that the deflections analysis can be treated by purely geometrical optics, consider a point P in the front grating of each moiré deflectometer with coordinates (x, y, z). If this point is projected to the self-image plane $z_i = z + Z_k$, then the coordinates of the projected point P_i are defined as $(x + \delta x_i, y + \delta y_i, z + Z_k)$, and the direction of this projection is defined as

$$cos\alpha = \frac{\delta x_i}{|PP_i|},\ cos\beta = \frac{\delta y_i}{|PP_i|},\ \cos\gamma = \frac{Z_k}{|PP_i|}, \tag{1}$$

where $\cos^2\alpha + \cos^2\beta + \cos^2\gamma = 1$, and the terms δx_i and δy_i represent the changes of the position. These terms are expressed in the following way:

$$\delta x_i(x, y) = |PP_i| \cos\alpha = \frac{\cos\alpha}{\cos\gamma} Z_k, \tag{2}$$

$$\delta y_i(x, y) = |PP_i| \cos\beta = \frac{\cos\beta}{\cos\gamma} Z_k. \tag{3}$$

The projection direction of the first grating of each deflectometer can be considered as the normal direction of the wavefront emerging of the turbulent atmosphere. Thus, using the paraxial approximation for light propagation, Eqs. (2) and (3) are written in terms of the gradients of the wavefront as

$$\delta x_i(x, y) = Z_k \frac{\cos\alpha}{\cos\gamma} = Z_k \frac{\partial U(x, y)}{\partial x}, \tag{4}$$

$$\delta y_i(x,y) = Z_k \frac{\cos\beta}{\cos\gamma} = Z_k \frac{\partial U(x,y)}{\partial y}, \tag{5}$$

where U is the propagated wavefront. The wavefront phase is given by $\phi(x,y) = \frac{2\pi}{\lambda}\ U(x,y)$, where λ is the wavelength.

The components of the AA fluctuations in the direction perpendicular to the rulings of the first grating (i.e. parallel to the corresponding moiré traces) are measured by the corresponding displacement of moiré traces. A particular local moiré fringe in the first deflectometer channel, for small θ, will translate along x according to[1,9]

$$\delta x_m(x,y) = \frac{\delta y_i(x,y)}{\theta} = \frac{d_m}{d}\delta y_i(x,y), \tag{6}$$

where d and d_m are the pitches of the gratings and the moiré fringe spacing, respectively. According to Eq. (6) the moiré fringe deviation is magnified by the factor $\frac{d_m}{d}$ or by the inverse of the angle θ. The wavefront tilt in the direction y at the point (x,y), then, relates to local moiré fringe displacement by

$$\frac{\partial U(x,y)}{\partial y} = \frac{d}{d_m Z_k}\delta x_m(x,y). \tag{7}$$

For a plane-wave with tilt, all the moiré fringes will translate by this amount but there will be no change in the fringe orientation. By the same token for the second channel, for the wavefront tilt in the direction x at the point (x,y), we obtain:

$$\frac{\partial U(x,y)}{\partial x} = \frac{d}{d_m Z_k}\delta y_m(x,y). \tag{8}$$

Therefore, the components of the AA fluctuations along the directions perpendicular to the lines of the gratings - parallel to the moiré traces - are derived. Experimentally, the traces of moiré fringe maxima were determined to within one pixel accuracy (for more details see our previous works[9,10]) and then fluctuations of the AA across the wavefront have been deduced.

3. WAVEFRONT RECONSTRUCTION

For the proposed wavefront sensor presented in the last section, a reconstruction of wavefront from the measurements is required. The general problem is the determination of the wavefront phase from a map of its gradient. Algorithmically, this involves the calculation of a surface by an integration-like process. The reconstruction problem can be expressed in a matrix-algebra framework. The unknowns, a vector $\emptyset$ of N phase values over a grid, must be calculated from the data, from a measurement vector $\mathbf{S}$ of M elements of wavefront slopes in two directions. The following general linear relation is thus obtained

$$\emptyset = \mathbf{BS}, \tag{9}$$

where $\mathbf{B}$ is the so-called reconstruction matrix.[11]A number of techniques are available to derive $\mathbf{B}$.[12–15] A linear model of wavefront sensor allows the linking of the measurements $\mathbf{S}$ to the incoming wavefront or its phase. The matrix equation between $\mathbf{S}$ and $\emptyset$ reads as

$$\mathbf{S} = \mathbf{A}\emptyset, \tag{10}$$

where $\mathbf{A}$ is called the interaction matrix. For the proposed two channel moiré deflectometer wavefront sensor, we have used Hudgin's and Frid's discretization.[12,13] For the geometry of discretization, the interaction matrix is determined, then the reconstruction matrix is obtained.

In order to perform the wavefront reconstruction from the measured moiré patterns, we consider the displacement of each moiré fringe trace respect to its reference position, which represents an estimate of the local x-slope or y-slope of the wavefront phase ϕ and the corresponding wavefront surface $U(x,y)$.

In practice, by considering two sets of the vertical and horizontal moiré traces of a frame in one x-y coordinate system, the intersection points of the vertical and the horizontal traces are determined. X-slope and y-slope of the wavefront are deduced from displacement of the intersection point in successive frames.

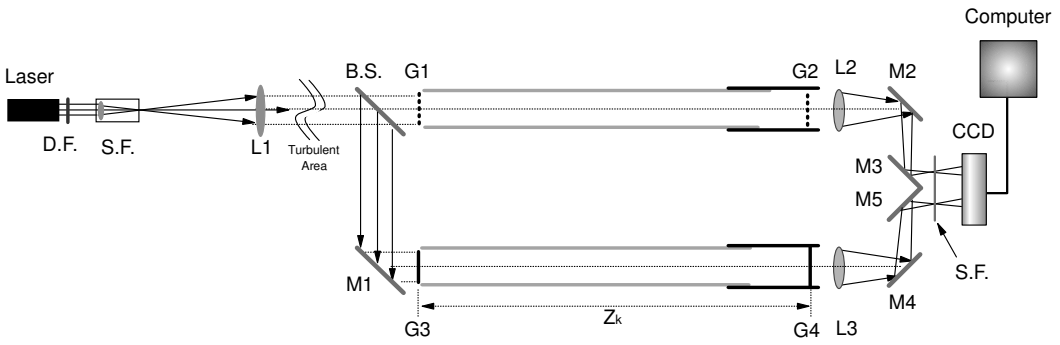

Figure 1. Schematic diagram of the experimental setup. G, L, M, and $S.F.$ stand for the gratings, lenses, mirrors, and spatial filters respectively. $D.F.$, $B.S.$ and Z_k stand for the neutral density filter, beam splitter, and talbot distance, respectively.

4. EXPERIMENTAL RESULTS

A schematic diagram of the experimental setup is shown in Fig. 1. The laser beam passes through a spatial filter, $S.F.$, and is collimated by the lens $L1$. It then passes through a turbulent area. Turbulence is produced over the path by a heater as the experiment was performed in the laboratory (indoor turbulence). By an amplitude beam splitter the laser beam splits into two beams. Each beam strikes the first gratings, $G1$ and $G3$, of the respective moiré deflectometers. The second gratings of the moiré deflectometers $G2$ and $G4$ are installed at a distance of 34.5 cm from the corresponding first gratings $G1$ and $G3$, respectively. Using lenses $L2$ and $L3$ and mirrors $M2$, $M3$, $M4$ and $M5$, images of the moiré patterns are projected on a CCD camera. These moiré patterns have the same size on the CCD camera and do not overlap. Unwanted spatial frequencies in the moiré patterns are removed in the focal plane of lenses $L2$ and $L3$ using a suitable spatial filter.

The CCD camera records successive moiré patterns and stores them in a computer. The identical gratings $G1$, $G2$, $G3$ and $G4$ have a ruling period of 1/10 mm and dimensions 20 mm $\times$ 20 mm and are installed on two parallel optical rails of changeable length to choose the desired Talbots distance. The grating holders are held on rotary mounts which can rotate about the optical axis for adjustment of the angle between the gratings. After alignment of the setup, the beam intensity was reduced by a neutral density filter to a level below the saturation level of the CCD. The moiré fringes were recorded at a sampling rate of 50 frames/s with a CCD camera, model PCO.1200hs, and fed to the PC. In the described experiments, the digitized frames consist of 468×1081 pixels. The moiré patterns of each channel consist of about 414×400 pixels. d_m was covered by 69 pixels in the first channel (for the vertical moiré fringes) and it was covered by 84 pixels in the second channel (for the horizontal moiré fringes).

Several sets of experimental data corresponding to different turbulence conditions were recorded and digitized with an image grabber. Successive images of moiré patterns at different times in the presence of turbulence are shown in Fig.2. These patterns were recorded at time intervals of 0.04 sec and is a typical set of measurements performed on July 2, 2009. The total data was collected in 5 s and contained 250 frames.

Two typical recorded frames in the absence of turbulence (non perceptible turbulence) (a), and in the presence of turbulence, (b), are shown in Fig.3. Each frame consists of two sets of orthogonal moiré patterns. Two components of the AA fluctuations are obtained from displacement of these orthogonal moiré patterns in successive frames. Traces of the moiré fringe maxima are specified to within one pixel accuracy. For more details see our previous work.[9,10,16] In Fig.4 and 5 the moiré fringes in the vertical and horizontal directions respectively without and with turbulence are shown in (a) and (d). The corresponding low-frequency illumination distribution are shown in (b) and (e). Derived traces of the bright moiré fringes are shown in (c) and (f). In Fig.6 all of the traces of the bright moiré fringes without air turbulence (green traces) and with air turbulence (red traces) are plotted. For the frames in Fig.3 (a) and (b), the intersection points of the traces are determined. Direction and magnitude of displacement of intersection points in the two frames are calculated and is shown in Fig.7. A larger shift is visualized by a larger length of the arrow. The phase distortion can be clearly seen as a

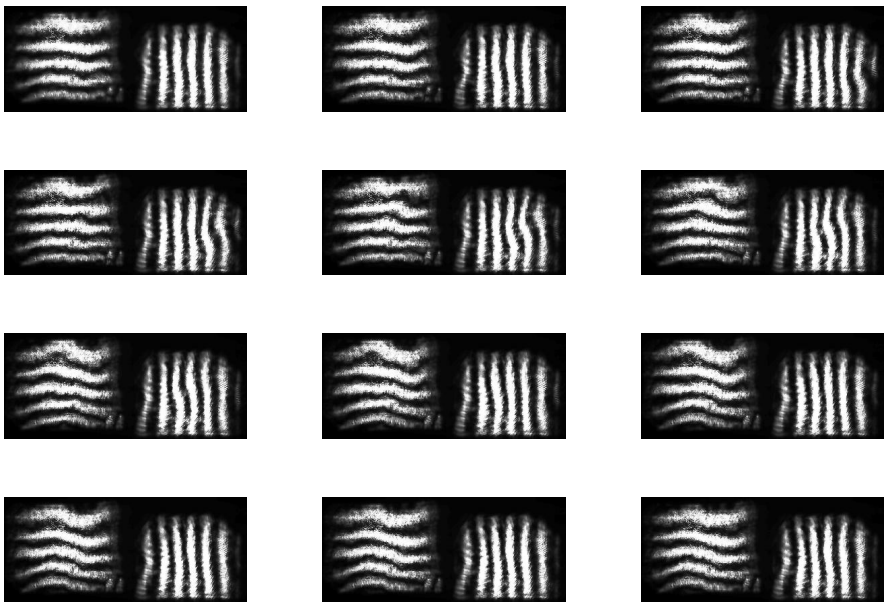

Figure 2. Successive frames of moiré patterns recorded at the time intervals of 0.04 sec. in the presence of turbulence.

varying shift of the moiré fringes in the direction perpendicular to their directions. From the magnitude of the displacements in x and y directions and by applying Eqs. (7) and (8) the wave-front slope in the corresponding directions were obtained.

In the described experiments, in order to perform the wavefront reconstruction from the measured wave-front slopes, we have used Hudgin's discretization.[12,13] For the geometry that we have used, the interaction matrix, **A**, and the reconstruction matrix, **B**, are derived. Using Eq. (9) and the measurement vector, **S**, of wavefront slopes in two directions, the desired wavefront is obtained. Reconstructed wavefront surface plot, corresponding to distortions generated by air turbulence in a region of $20mm \times 20mm$ are shown in Fig.8.

5. CONCLUSION

In this paper we presented a new method for wavefront sensing. Taking advantage of two channel arrangement employing moiré deflectometry we have measured two component of the AA fluctuation across the wavefront. By measuring the moiré fringes distortions of both channels, the information content of the phase of the wavefront can be obtained.

The moiré deflectometry overcomes the technical difficulties of the Schlieren and Shack-Hartmann techniques. Another advantage is that the method is implementable in a compact and very low cost form. By using two channel moiré deflectometers we have overcome some of disadvantages of moiré deflectometry using crossed gratings.

The moiré deflectometers can be performed with either amplitude or phase gratings. The later have an advantage, because there is no energy loss. This is helpful when sensing wavefront coming from a celestial object.

The sensitivity of detection is adjustable by merely changing the distance between two gratings and relative grating angle. This overcomes another deficiency of the Shack-Hartman sensors in that they require expensive retrofitting to change sensitivity. Besides, in the moiré deflectometry, the measurement is relatively insensitive to the alignment of the beam into the device.

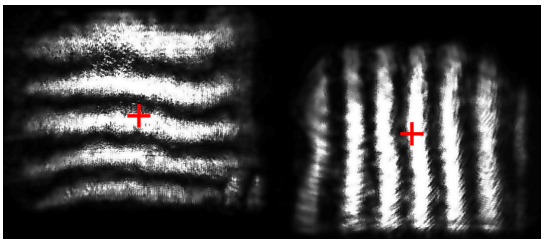

(a)

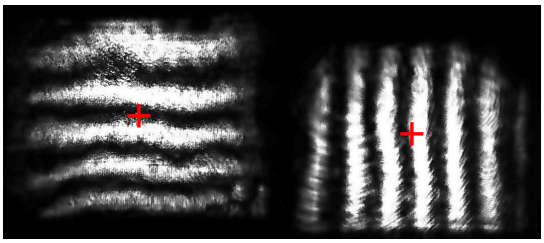

(b)

Figure 3. Typical recorded frames in the absence of turbulence (non perceptible turbulence), (a), and in the presence of turbulence (b). Each frame consists of two sets of orthogonal moiré patterns. " + " show center of the horizontal or vertical moiré patterns.

Since only tilts are measured the Shack-Hartmann can not detect discontinuous steps in the wavefront. As in this method AA fluctuations are measured across the traces, discontinuous steps in the wavefront will be detectable.

This method is applicable to measuring atmosphere induced wavefront distortions in the light coming from celestial objects.

In this method similar to the Shack-Hartmann method data manipulation to retrieve quantitative wavefront information is a time-consuming process.

ACKNOWLEDGMENTS

Saifollah Rasouli would like to acknowledge Professor Yousef Sobouti for his valuable support for accomplishing the research described in this paper.

REFERENCES

[1] K. Patorski and M. Kujawińska, *Handbook of the moiré fringe technique*, Elsevier, Amsterdam, 1993.

[2] Ricardo Legarda-Saenz, "Robust wavefront estimation using multiple directional derivatives in moiré deflectometry", *Optics and Lasers in Engineering* **45**, pp. 915–921, 2007.

[3] J. A. Quiroga, D. Crespo, and E. Bernabeu, "Fourier transform method for automatic processing of moire deflectograms", *Opt. Eng.* **38**, pp. 974-982, 1999.

[4] Norberto H. Salama, D. Patrignani, L. D. Pasquale, and E. E. Sicre, "Wavefront sensor using the Talbot effect", *Optics & Laser Technology* **31**, pp. 269–272, 1999.

[5] Ch Siegel, F. Loewenthal, and L. E. Balmer, "A wavefront sensor based on the fractional Talbot effect", *Optics Communications* **194**, pp. 265–275, 2001.

[6] C. L. Hou, and J. Bai, "Wavefront Measurement for Long Focal Large Aperture Lens Based on Talbot Effect of Ronchi Grating", *Journal of Physics: Conference Series* **48**, pp. 1037–1041, 2006.

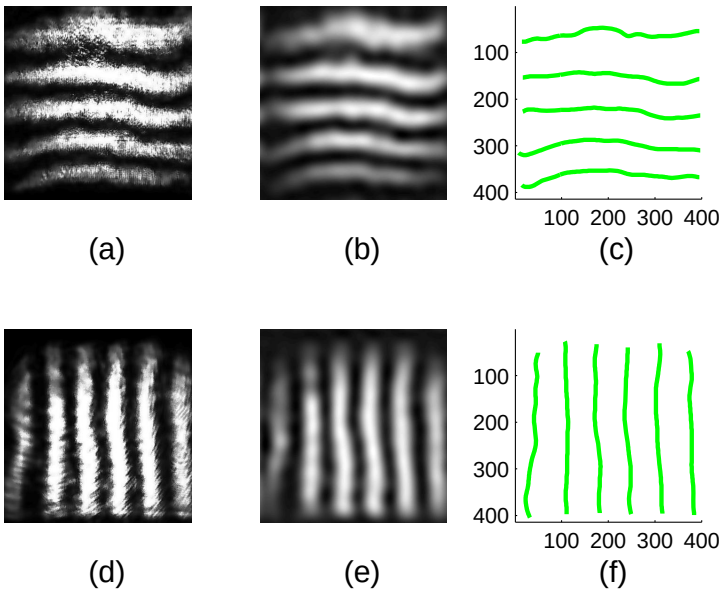

Figure 4. (a) and (d) typical moiré fringes in the horizontal and vertical directions without air turbulence, (b) and (e) the corresponding low-frequency illumination distribution. Derived traces of bright moiré fringes are shown in (c) and (f), respectively.

[7] G. Y. Yoon, T. Jitsuno, M. Nakatsuka, and S. Nakai, "Shack Hartmann wave-front measurement with a large F-number plastic microlens array", *Applied Optics* **35**, pp. 188–192, 1996.

[8] E. Hecht, and A. Zajak, *Optics*, Addison-Wesley, 1974.

[9] S. Rasouli, and M. T. Tavassoly, "Application of moiré technique to the measurement of the atmospheric turbulence parameters related to the angle of arrival fluctuations," *Opt. Lett.*, **31**, pp. 3276–3278, 2006.

[10] S. Rasouli, and M. T. Tavassoly, "Application of the moiré deflectometry on divergent laser beam to the measurement of the angle of arrival fluctuations and the refractive index structure constant in the turbulent atmosphere," *Opt. Lett.* **33**, pp. 980–982, 2008.

[11] F. Roddier, *Adaptive optics in astronomy*, Cambridge university press, Cambridge, United Kingdom 1999.

[12] J. Herrmann, "Least-squares wave front errors of minimum norm," *J. Opt. Soc. Am.* **70**, pp. 28–35, 1980.

[13] B. R. Hunt, "Matrix formulation of the reconstruction of phase values from phase differences," *J. Opt. Soc. Am.* **69**, pp. 393–399, 1979.

[14] D. L. Fried, "Least-square fitting a wave-front distortion estimate to an array of phase-difference measurements," *J. Opt. Soc. Am.* **67**, pp. 370–375, 1977.

[15] W. H. Southwell, "Wave-front estimation from wave-front slope measurements," *J. Opt. Soc. Am.* **70**, pp. 998–1006, 1980.

[16] S. Rasouli, and M. T. Tavassoly, "Measurement of the refractive-index structure constant, C_n^2, and its profile in the ground level atmosphere by moiré technique,"in *Optics in Atmospheric Propagation and Adaptive Systems IX*, A. Kohnle,and K. Stein, ed., *Proc. SPIE* **6364**, pp. 63640G-1–11, 2006.

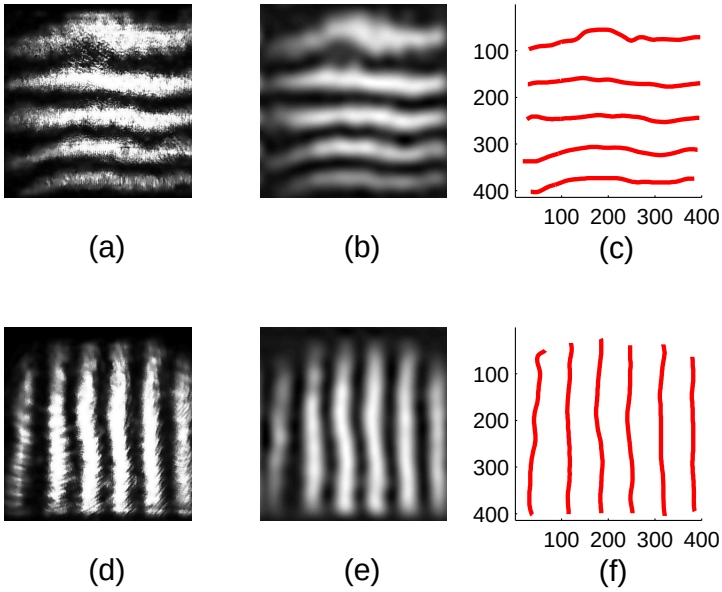

Figure 5. (a) and (d) typical moiré fringes in the horizontal and vertical directions with air turbulence, (b) and (e) the corresponding low-frequency illumination distribution. Derived traces of bright moiré fringes are shown in (c) and (f), respectively.

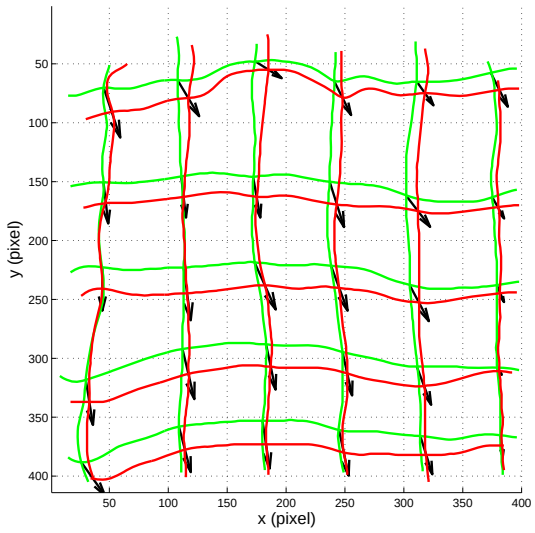

Figure 6. Traces of bright moiré fringes of both channel without air turbulence (green traces), and with air turbulence (red traces). Arrows show the displacements of the intersection points due to turbulence.

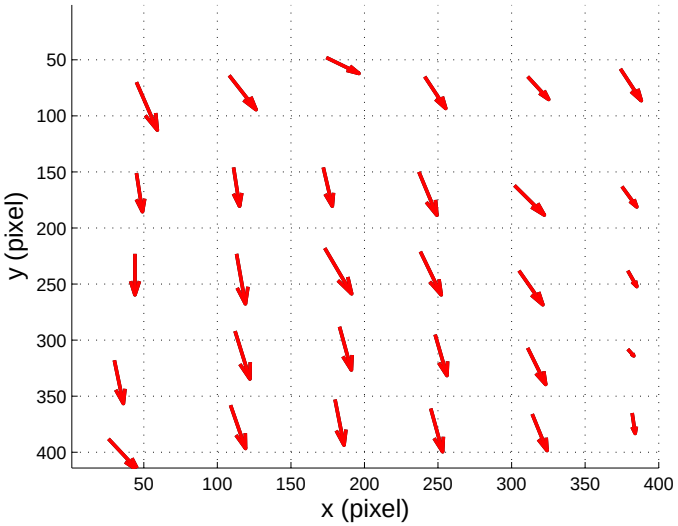

Figure 7. Direction and magnitude of the displacements of intersection points of moiré fringes. A larger shift is visualized by a larger length of the arrow.

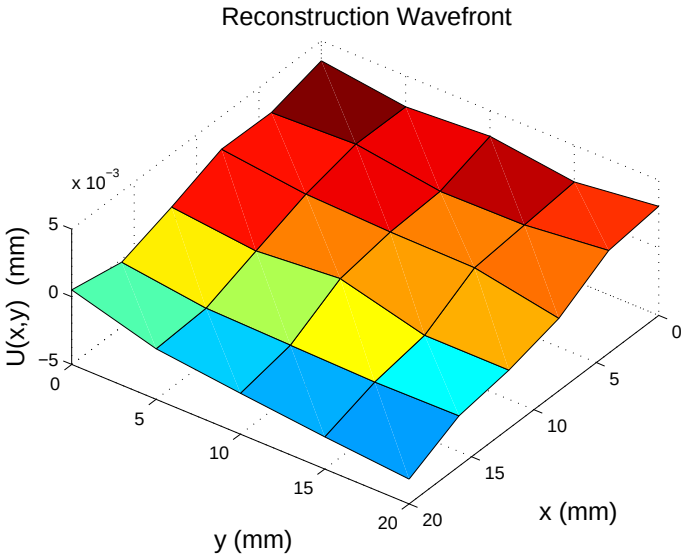

Figure 8. Reconstructed wavefront, surface plot, corresponding to distortions generated by air turbulence in a region of $20mm \times 20mm$.